Materials Science Forum
ISSN: 1662-9752, Vol. 1184, pp 43-52
doi:10.4028/p-06WuSM

Submitted: 2026-01-19
Revised: 2026-02-17
Accepted: 2026-02-21
Online: 2026-04-14

Numerical Analysis of Roughness Transfer Mechanism during Skin-Pass Rolling

Hamed Aghajani Derazkola[1,a*], Leon Jacobs[2,b], Stamatis Kiakidis[2,c], Ton van den Boogaard[1,d], Javad Hazrati[1,e]

[1]Nonlinear Solid Mechanics, Faculty of Engineering Technology, University of Twente, Enschede, The Netherlands

[2]Tata Steel, Research & Development, 1951 JZ Velsen-Noord, The Netherlands

[a*]h.aghajaniderazkola@utwente.nl, [b]leon.jacobs@tatasteeleurope.com, [c]Stamatis.Kiakidis@tatasteeleurope.com, [d]a.h.vandenboogaard@utwente.nl, [e]j.hazratimarangalou@utwente.nl

[*]corresponding author

Keywords: skin-pass rolling, roughness transfer, finite element model.

Abstract. Skin-pass rolling is a finishing process characterized by very small thickness reductions, primarily applied to control surface texture and mechanical properties of rolled steel strips. A key outcome of this process is the transfer of surface roughness from the work roll to the strip, which is governed by local contact conditions at the roll–strip interface. In this study, roughness transfer during skin-pass rolling of DX56 steel sheets is investigated using a combined macro–micro finite element modeling approach supported by pilot-mill experiments. Rolling trials were conducted to measure thickness reduction and resulting surface roughness under different rolling forces and entry tensions. A macro-scale rolling model was first employed to estimate effective friction coefficients by reproducing the experimentally observed thickness reductions for each rolling condition. These calibrated friction coefficients were subsequently applied in a micro-scale finite element model incorporating an electro-discharge textured (EDT) roll surface to analyze local contact pressure, plastic strain accumulation, and roughness transfer mechanisms. The results show that increasing rolling force leads to higher contact pressures, longer roll bites, and enhanced asperity-scale plastic deformation, resulting in increased roughness transfer. Entry tension modifies the stress distribution within the roll bite, which facilitates localized yielding without inducing plastic deformation prior to roll entry. The simulations capture the qualitative trends of surface roughness evolution observed experimentally, demonstrating the capability of the proposed finite element framework to analyze roughness transfer mechanisms in skin-pass rolling.

Introduction

Surface texture of cold rolled steel strips determines its visual appearance, paint ability and tribological behavior [1]. The texture is being printed on the strip surface by rolls with preferred surface roughness, in the skin-pass which is the last sequence of the steel sheet rolling. Therefore, a thorough mechanistic understanding of skin-pass rolling with the elastic-plastic deformation analysis at the asperity level is necessary to design and control the product surface texture using different process parameters [2-4]. Despite extensive research on conventional rolling, the process of roughness transfer from roll to strip has not yet been thoroughly addressed. In skin-pass rolling, the reduction in strip thickness is typically less than 3%. The primary deformation occurs at the strip surface [5]. Simulating roughness transfer in skin-pass rolling presents significant challenges due to the need for accurate material modeling, contact conditions, and precise handling of micro-scale roughness transfer with localized micro level fine meshes. Hence, there are a couple of studies in the literature focusing on analysis of skin-pass rolling. Kijima and Bay [6] discussed the difficulties of experiments and modeling of skin-pass and simplified the problem by adopting a plane strain model to study the effect of friction in skin-pass rolling. They show that skin-pass rolling involves an extended sticking region producing highly inhomogeneous deformation, and that plane-strain

upsetting provides an accurate surrogate for studying these mechanisms. Experiments confirmed FEM predictions of sticking/sliding boundaries, validating the modelling approach for high-friction, small-reduction rolling. In their next work [7], they applied only normal loads with no tangential sliding in a FE model to make texture on the strip surface and compared with skin-pass rolling experiments. They reported that both tool roughness and pitch strongly affect roughness transfer, with smaller roughness and larger pitch producing higher transfer. Kijima and Bay [8] applied tangential shear after normal load (in two steps) in their next study to make the analysis more realistic and closer to the skin-pass rolling. The study concludes that tangential displacement (both in sticking and sliding regions) significantly increases roughness transfer, meaning that pure normal-loading models underestimate surface deformation in practical dry skin-pass rolling. The work verifies FE predictions with experiments and shows a pronounced roughness peak at the sliding–sticking boundary. Bünten et al. [9] concludes that the developed FE model (validated through detailed upsetting tests and applied to temper-rolling conditions) can accurately predict the microscopic transfer of deterministic roll-surface structures, reproducing both penetration and reverse-extrusion mechanisms observed experimentally. It further shows that, for the geometries and elongations studied, the frictional coefficient does not need to be prescribed explicitly because the microscopic surface topography alone governs the effective frictional response in the simulations.

This work presents macro- (without roll roughness) as well as micro-scale (with roll roughness) analyses of skin-pass rolling by a FE model. The effects of process parameters such as rolling force and strip tension on the contact pressure and strip velocity at the roll bite are presented. Afterwards, the macro-scale model is adjusted to include simplified micro-geometry of EDT asperities on the roll. The model is used to investigate the effect of rolling force and entry tension on the transferred roughness on the strip.

Experimental Procedure

The rolling experiments and sample preparation were conducted using the Multi mill (pilot test) at Tata Steel, Netherlands. The material used in this study was DX56 steel sheet with initial thickness of 3 mm which is cold rolled to 0.6 mm before skin-pass rolling. In these experiments, the DX56 steel strip was intentionally not annealed and therefore remained in a full-hardened condition before skin pass rolling. This choice was made deliberately, as the material behavior of full-hardened steel is more straightforward to characterize than that of annealed material. Prior to the skin-pass rolling stage, the material properties were measured by uniaxial tensile test. A series of trials were conducted at Tata Steel, and the effects of rolling force and entry/exit tension on the strip thickness reduction were evaluated (Table 1). In these experiments, a 195mm roll radius was selected and rolling speed of 2 m/s was used. These results are used for the validation of the FEM simulation.

Table 1. Selected process parameters (experiments) for evaluation of FEM model.

Sample	Strip thickness	Entry tension	Exit tension	Rolling force	Thickness reduction
1	0.6mm	200MPa	55MPa	300kN	0.291%
2	0.6mm	200MPa	55MPa	900kN	1.5%
3	0.6mm	300MPa	55MPa	900kN	1.75%

The surfaces of the skin-pass rolled sheets (Samples 1, 2, and 3) were evaluated using a confocal microscope (Sensofar) to characterize their surface roughness properties. Measurements were performed at both the edges and the center of each sheet.

Finite Element Model

The material properties were measured experimentally and used for simulation. Bergstrøm-van Liempt (BvL) hardening model (stress-strain curve) was used to estimate flow stress [10]. Before reaching the skin-pass rolling stage, the DX56 steel sheets undergo several preliminary deformation steps, which introduce pre-strains that affect the material behavior during skin-pass rolling. The von-Mises yield criterion is used for this steel during the simulation.

In this research, ABAQUS 2023 software is used to develop the plane strain finite element model of the skin pass rolling. The model used in this study is force-controlled, meaning that the rolling force is applied to the sheet through an elastic work roll. A midplane symmetry boundary condition is also imposed at the bottom of the strip. During simulation, for the vertical interaction, a hard contact model with the augmented Lagrange method was applied. For the tangential interaction, the penalty method was used. The rolling forces and the entry tension (ET) range were selected based on the experiments. In this simulation, the roll force and the entry and exit tensions were defined as input parameters, while the thickness reduction (measured experimentally) was the output variable. Using this approach, the coefficient of friction (COF) at the interface was calibrated to obtain the value that reproduces the experimentally observed thickness. To simulate the roughness transfer, an electro-discharge texturing (EDT) single event geometry was taken from reference [11] and modeled on the roll for simulation. Image of indent dimension is presented in Figure 1a. To reduce computation time, only seven indents were modeled on the work roll while still capturing the relevant interface behavior. To mesh the model, various mesh ratios and sectioning approaches were tested on both the roll and the strip to find the optimal mesh for convergence. The top surface region of the sheet in direct contact with the EDT indentation was discretized using a locally refined mesh. Adaptive remeshing was implemented within Abaqus/Standard during the cold rolling simulation to control element distortion and ensure stable convergence of the implicit solution. To accurately describe the contact and deformation of the roll, 7 rows of elements, each with double the mesh size of the strip were placed along the outer circumference of the roll. The element type used was CPE4 (plane strain). Figure 1b shows the mesh domain in this study.

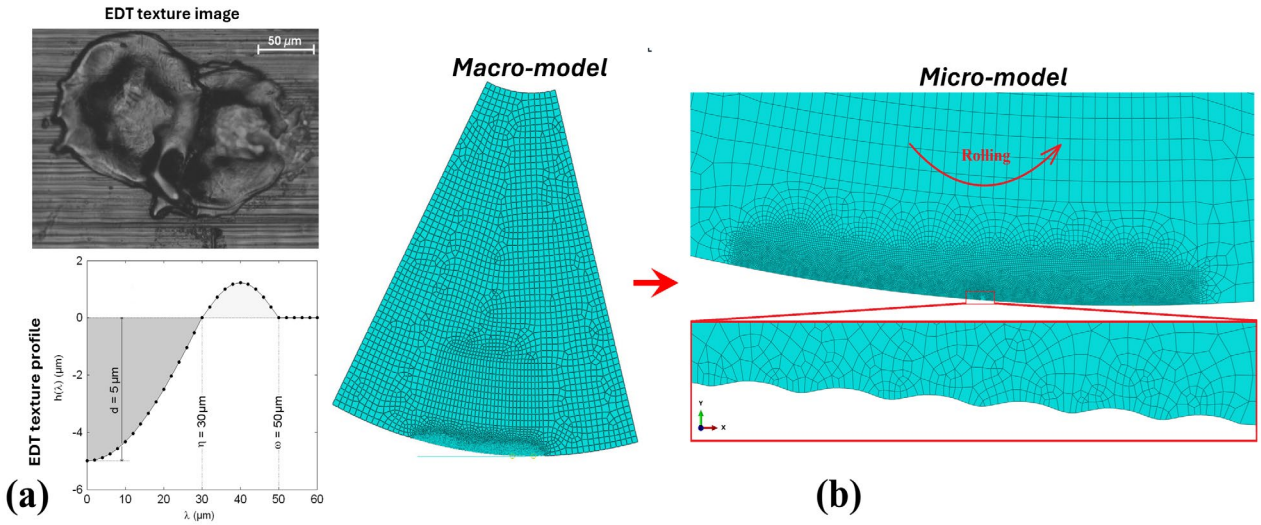

Fig. 1. (a) Single EDT geometry [10], and (b) mesh domain of skin pass rolling.

Macro-scale model

Macro-scale model of rolling process (excluding the roll texture) is used to reproduce the experimental results by calibrating the coefficient of friction (COF). The calibrated COFs later are used in micro-scale model to simulate roughness transfer in skin pass rolling. Figures 2a and 2b show contact pressure and surface nodal displacement of sheet at roll bite, respectively. The latter is a good approximation since it has been shown that ploughing effects of the texture on friction at the roll bite can be neglected [12]. For sample 1, an effective COF of 0.073 reproduces the experimentally observed thickness reduction. Under these conditions, the maximum contact pressure reaches 0.72 GPa and the roll bite length is approximately 3.6 mm. Increasing the rolling force from 300 kN (Sample 1) to 900 kN (sample 2) leads to a pronounced increase in contact pressure and a significant extension of the roll bite. For sample 2, an effective COF of 0.139 is required, leading to a peak contact pressure of 1.35 GPa and a roll bite length of 6.0 mm.

In samples 2 and 3, the rolling force was kept constant at 900 kN, while the entry tension was increased from 200 MPa to 300 MPa. The simulations show that increasing the entry tension slightly

extends the roll bite length to 6.2 mm while reducing the peak contact pressure to 1.32 GPa. The calibrated COF for sample 3 is 0.135, which is slightly lower than that obtained for sample 2 (0.139). The calibrated COF values should be interpreted as effective friction coefficients reflecting the pressure-dependent tribological response of the roll–strip interface. At higher rolling forces, increased contact pressure promotes work roll flattening, increases the real area of contact, and leading to higher frictional resistance. Consequently, an increase in the effective COF with rolling force is consistent with the known behavior of skin-pass rolling under high contact pressures.

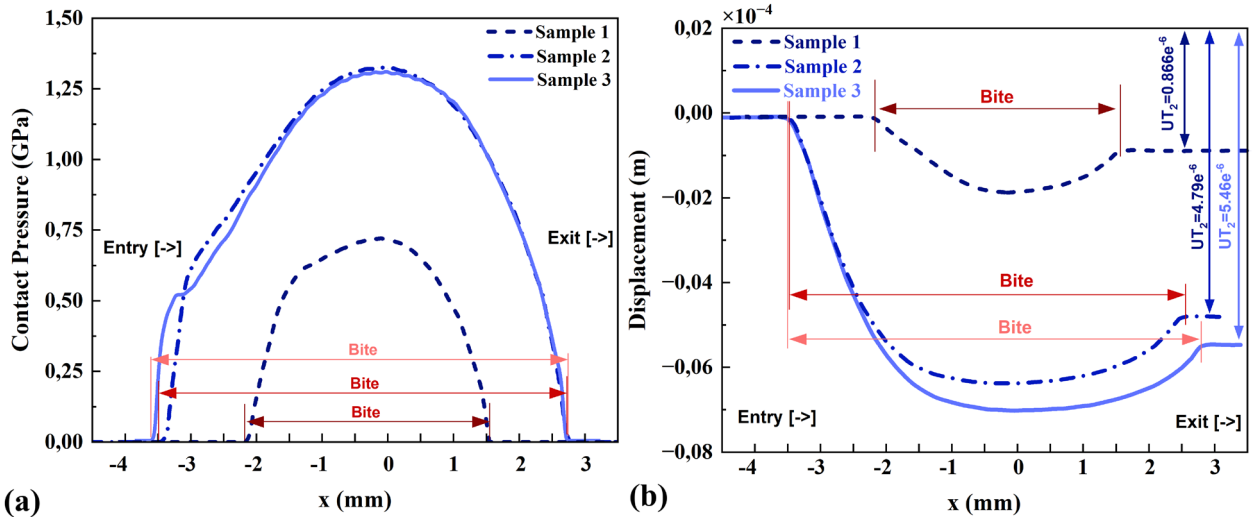

Fig. 2. (a) Contact pressure distribution and (b) surface nodal displacement (UT2) along the roll bite for samples 1 (300kN-200MPa), 2 (900kN-200MPa) and 3 (900kN-300MPa) obtained from macro-scale finite element simulations. The spatial coordinate x is defined along the rolling direction, with x = 0 at the roll centerline; negative values indicate the entry side and positive values the exit side of the roll bite. Arrows indicate the roll bite length for each condition.

Entry tension was found to have a limited influence on the magnitude of the contact pressure but affected its distribution along the roll bite. Higher entry tension slightly reduced the peak contact pressure, shifted it toward the exit side, and extended the roll bite length [13]. This behavior is attributed to the elastic tensile stress introduced prior to roll entry, which alters the stress state of the strip and modifies the equilibrium between normal pressure and frictional shear within the roll bite, thereby shifting the neutral point downstream [14]. Although the peak contact pressure decreases, plastic deformation is not inhibited; instead, yielding is facilitated under the combined action of normal pressure and tensile stress, leading to a redistribution of deformation along the roll bite. Table 2 summarizes the simulation results and compares them with the experimental data. The experimental thickness reductions for Samples 1, 2, and 3 are 0.291%, 1.50%, and 1.75%, respectively. Based on the surface nodal displacement (UT2) obtained from the simulations, the corresponding thickness reductions for Samples 1, 2, and 3 are 0.288%, 1.59%, and 1.82%, respectively.

Table 2. FEM model results and comparison with experiments.

Sample	Experimental thickness reduction	Simulation thickness reduction	Thickness reduction error	Roll bite length	Maximum contact pressure	COF
1	0.291%	0.288%	1.1%	3.6mm	0.719GPa	0.073
2	1.5%	1.59%	5.7%	6.0 mm	1.35GPa	0.139
3	1.75%	1.82%	3.9%	6.2mm	1.32GPa	0.135

Micro-scale model

The FEM results revealed distinct trends in contact pressure at both the micro and macro scales during skin-pass rolling, particularly regarding the shape and magnitude of the pressure distribution. Figure 3a shows a representative contact-pressure distribution from the micro-scale model. As outlined in the modelling section, only seven indents were included on the work roll to reduce computational cost. As expected, the contact pressure in the indented zone (representing the EDT events) is higher than that in the smooth regions of the roll surface. A magnified view of the pressure field around the seven indents is provided in Figure 3b. The contact pressure exhibits a periodic pattern, rising from zero to a local maximum at each indent. The zero-pressure regions correspond to locations where the roll and strip are not in contact. The first (leading) and last (trailing) indents show lower peak pressures than the central indents, which is a consequence of the roll geometry definition in the model and should be disregarded.

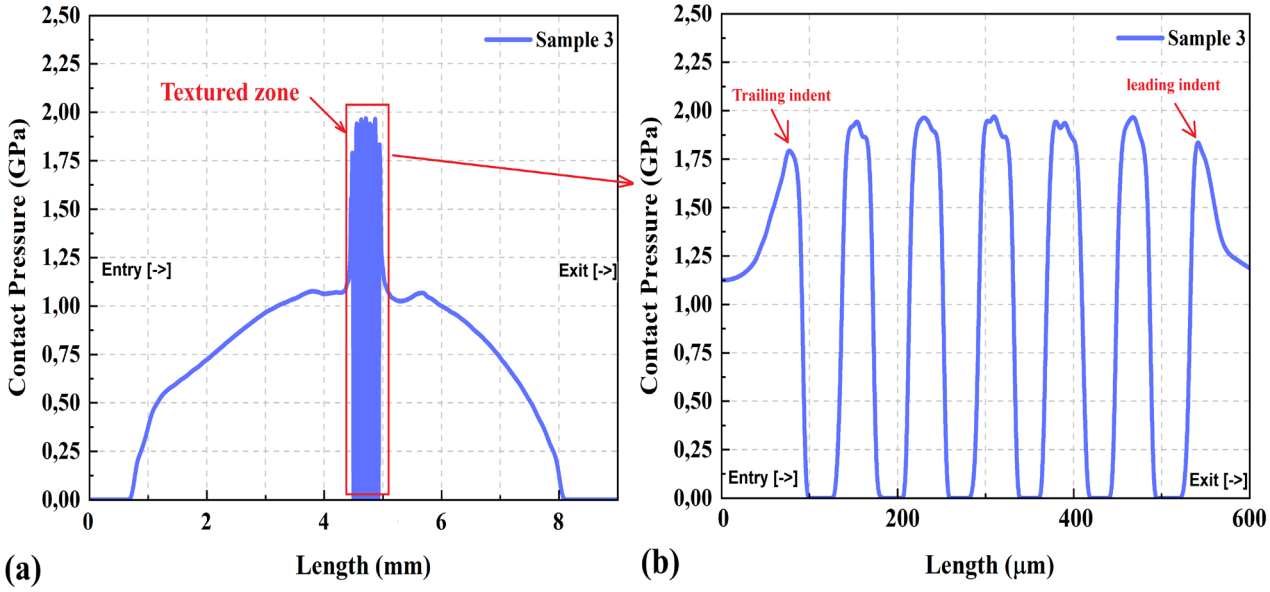

Fig. 3. (a) Contact pressure of Sample 3 (900kN-300MPa) at micro-scale, (b) high magnification contact pressure at the textured zone.

Figure 4a presents the FE simulation results of the contact pressure for the micro-scale model. As mentioned before, in the macro-scale model, the deformed roll maintained continuous contact with the strip along the roll bite. In contrast, for the textured roll at the micro scale, the contact area between the roll and the strip within the roll bite was discontinuous. As shown in Figure 4a, the rims of the textures were in direct contact with the strip, while the strip material did not directly contact the craters. The degree of contact between the roll and the strip depends on the process parameters such as rolling force and strip tension [15]. The effects of rolling force and entry tension on the contact pressure and normal stress for a single EDT event are illustrated in Figure 4b. In this section, the length is expressed in micrometers, representing the contact length between one EDT event and the strip. At the macro scale, the maximum contact pressures at the roll bite for Samples 1, 2, and 3 were 0.719 GPa, 1.35 GPa, and 1.32 GPa, respectively. In contrast, at the micro scale, the limited contact area at the indent–strip interface led to a significant increase in the local contact pressure. The FEM results show that the maximum contact pressures at the rim–strip contact area for Samples 1, 2, and 3 were 1.51 GPa, 2.06 GPa, and 1.99 GPa, respectively.

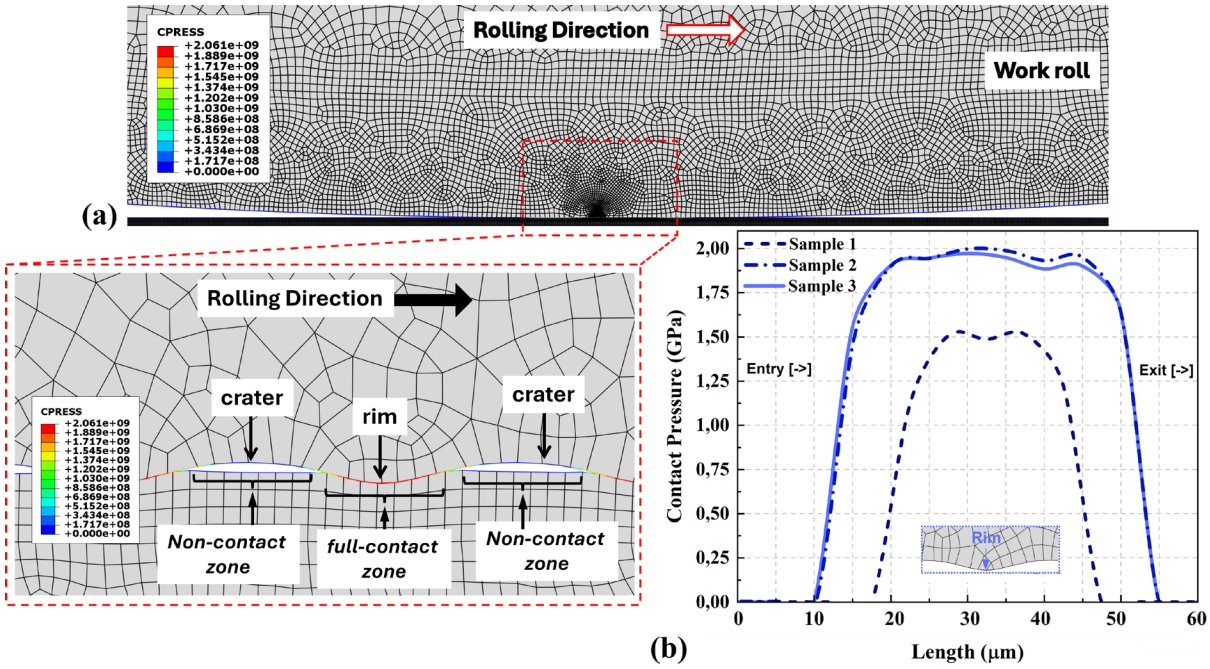

Fig. 4. FEM results of contact pressure at micro-model (Sample 3 (900kN-300MPa) and (b) contact pressure of single indent for Sample 1 (300kN-200MPa), Sample 2 (900kN-200MPa) and Sample 3 (900kN-300MPa).

For a more comprehensive understanding, Figures 5a and 5b present the complete distribution of contact pressure and normal stress (S22) for Sample 2 at the roll bite. As a result of the periodic repetition of EDT textures on the work roll surface, both the full-contact and non-contact regions are periodically reproduced along the contact length. Meanwhile, the maximum contact pressure and normal stress occurring at the rims of the textures remain nearly constant.

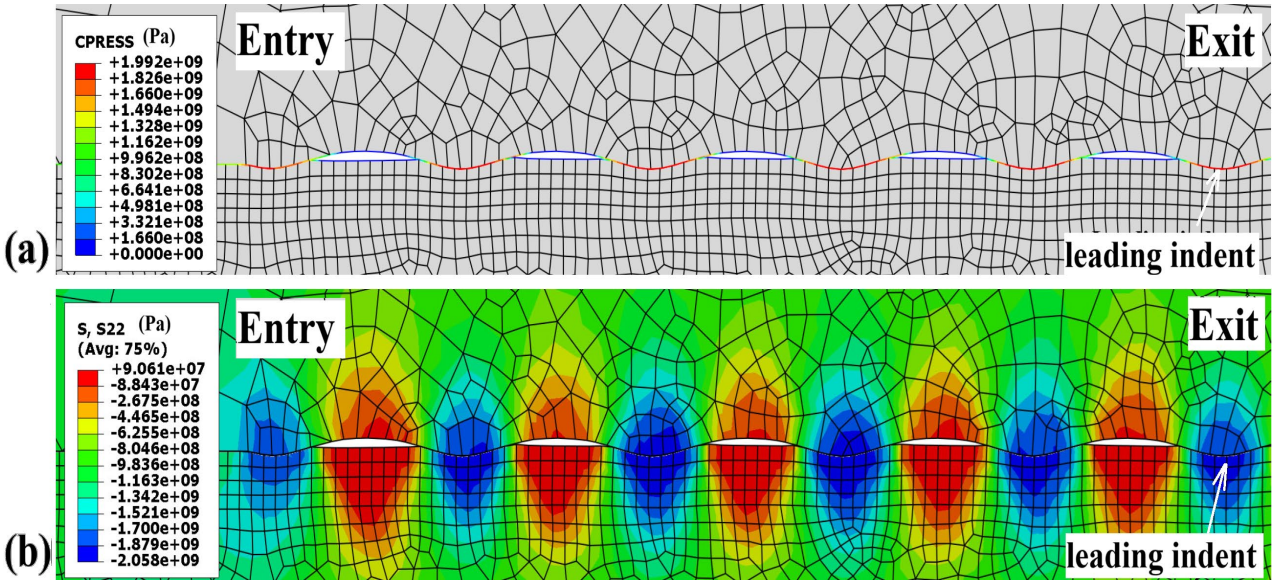

Fig. 5. (a) FEM results of contact pressure and (b) normal stress of micro-scale at Sample 2 (900kN-200MPa).

Figure 6a illustrates the distribution of equivalent plastic strain (PEEQ) for Sample 2 as a representative case. The PEEQ is highly localized near the strip surface and exhibits pronounced maxima at the leading and trailing edges of the surface indents. This localization reflects the non-uniform contact conditions at the roll–strip interface, where micro-scale variations in contact pressure and friction govern the local plastic flow; indentation and extrusion of material. Figure 6b presents the evolution of PEEQ along the rolling direction for all three samples under different rolling force and entry tension conditions. The PEEQ distribution closely follows the corresponding micro-scale

contact pressure profile, confirming that local pressure maxima dominate strain accumulation during skin-pass rolling. The deformation pattern further confirms that ploughing of the indents on the strip surface is negligible for the investigated rolling conditions. An increase in rolling force leads to a higher mean contact pressure, which amplifies local pressure peaks at the indent edges and consequently increases the PEEQ. The maximum PEEQ values for Samples 1, 2, and 3 were 0.169, 0.28, and 0.375, respectively.

A systematic difference between the leading and trailing indents is also observed, with higher PEEQ values occurring at the trailing edge (figure 6b). This asymmetry arises from material pile-up within the crater region during roll passage. The pile-up (extrusion in the crater) increases the effective contact length and enhances adhesive friction drag, resulting in a higher accumulated plastic strain at the trailing indent compared to the leading one. Entry tension exerts a significant influence on the PEEQ distribution by modifying the local stress state at the roll–strip interface towards pure shear and therefore reducing the yield stress of the material.

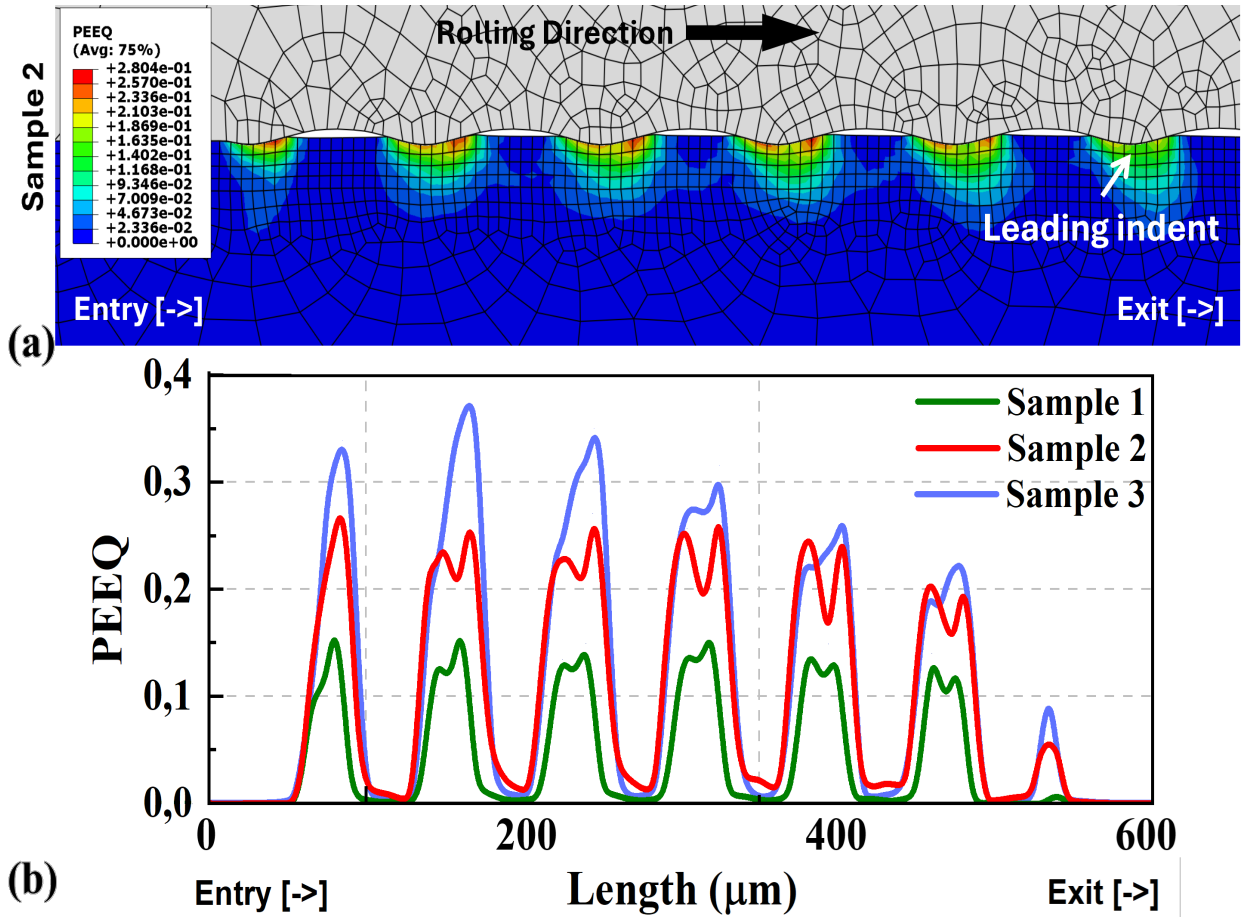

Fig. 6. (a) FEM results of EDT textures PEEQ for Sample 2 (900kN-200MPa) and (b) comparison of PEEQ for all Samples.

Figure 7 presents the finite element results of strip surface deformation after rolling with textured work rolls for sample 2. The corresponding surface profiles of samples 1, 2, and 3, expressed in terms of surface nodal displacement (µm), are shown in Figure 7, highlighting the differences in surface roughness morphology under varying rolling force and entry tension conditions. The results demonstrate a pronounced influence of rolling force on the shape of the crater region. At higher rolling forces, the crater exhibits a more pronounced frustum-like profile, indicating enhanced filling of the roll-induced surface features. This behavior is associated with increased contact pressure and frictional traction at the roll–strip interface, which promote localized plastic flow and material displacement into the crater. In contrast, at lower rolling forces, the lower contact pressure limits plastic flow, resulting in a flatter and less developed crater morphology.

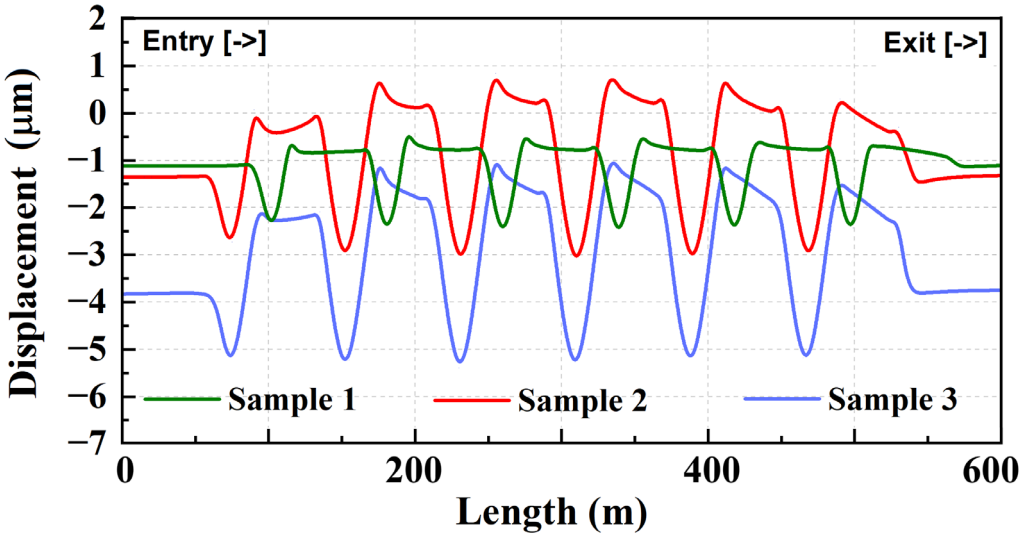

Fig. 7. Comparison of surface nodal displacement (deformation) between experiments and simulation.

For evaluation of FEM results the arithmetical mean surface roughness (Ra) of deformed surface is calculated by:

$$R_a = \frac{1}{N}\sum_{i=1}^{N}|Z_i - \bar{Z}| \quad (1)$$

where Z_i denotes the measured surface height at i-th measured point of the surface profile, $\bar{Z}$ is the mean height over the evaluation length, and N is the total number of measurement points used to compute the arithmetical mean roughness. The combined effects of rolling force and entry tension on the micro-scale Ra of the strip are shown in Figure 8. The calculated Ra values exhibit a trend consistent with that of thickness reduction. The average simulated Ra values for Samples 1, 2, and 3 were 0.39μm, 0.94μm, and 1.15μm, respectively. Correspondingly, the experimental results obtained from the top surface of the DX56 sheet produced under the same rolling conditions showed Ra values of 0.91μm, 1.80μm, and 2.04μm for Samples 1, 2, and 3, respectively. It is important to note that the Ra computed from the FEM results corresponds to a simplified, homogeneous, and periodic EDT texture represented under plane-strain conditions, implying infinitely wide asperities in the transverse direction. In contrast, the work-roll roughness in the pilot mill is stochastic and three-dimensional, which explains the quantitative discrepancy between the simulated and experimental Ra values. Nevertheless, the FEM results correctly capture the qualitative trend of increasing Ra with increasing rolling force and entry tension.

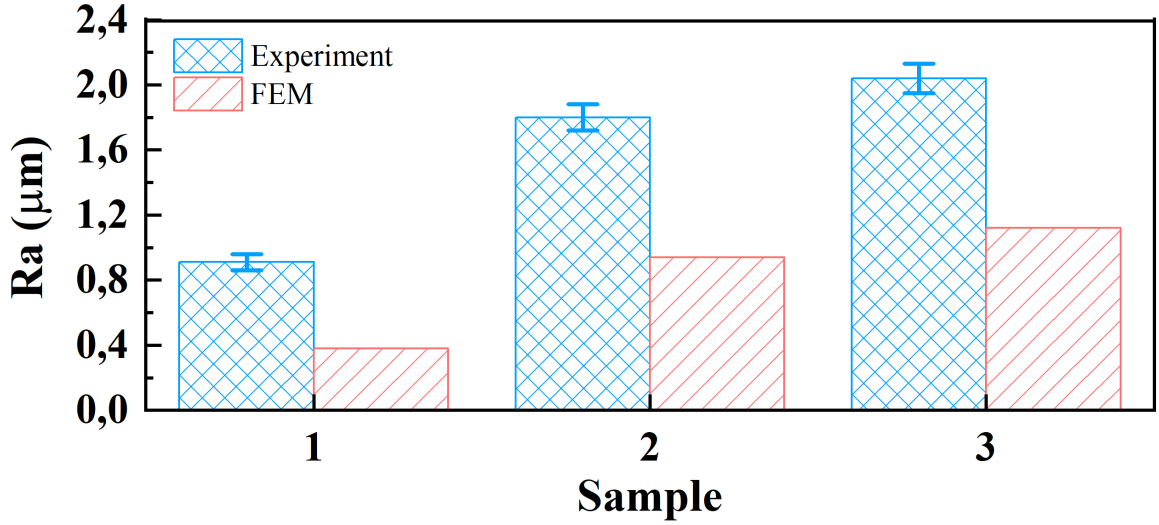

Fig. 8. Comparison of Ra between experiments and simulation.

Summary

This study investigated the influence of rolling force and entry tension on roughness transfer during skin-pass rolling using a combined macro–micro finite element framework supported by pilot-mill experiments. A macro-scale rolling model was first employed to reproduce experimentally observed thickness reductions by calibrating friction coefficients for each rolling condition. These calibrated friction values were subsequently applied in micro-scale simulations incorporating an EDT-type surface geometry to analyze local contact conditions and asperity-scale deformation.

The numerical results show that increasing rolling force leads to higher contact pressures, longer roll bites, and larger plastic deformation at the asperity scale, resulting in enhanced roughness transfer. Entry tension was found to modify the stress state within the roll bite by superimposing a tensile stress on the strip, shifting the neutral point and promoting localized plastic deformation. Although rolling force, entry tension, and friction are inherently coupled in the experimental conditions considered, the simulations capture their combined influence on roll bite geometry, contact conditions, and surface deformation behavior.

The micro-scale model successfully reproduces key qualitative trends observed experimentally. Quantitative differences between simulated and measured Ra values are attributed to the simplified and periodic representation of roll roughness in the numerical model compared to the complex stochastic texture of the industrial work rolls. Future work will focus on incorporating measured roll-surface topographies, lubrication effects, and more advanced constitutive description of strip material to further improve the predictive capability of the model for industrial skin-pass rolling applications.

References

[1] F. J. Huertos, F. Clarysse, and M. Vermeulen, ‘Identification of the paint process for steel sheet applications’, Wear, vol. 266, no. 5–6, pp. 523–526, 2009.

[2] M. Vermeulen and J. Scheers, ‘Micro-hydrodynamic effects in EBT textured steel sheet’, Int. J. Mach. Tools Manuf., vol. 41, no. 13–14, pp. 1941–1951, 2001.

[3] D. P. Gruber, M. Buder-Stroisznigg, G. Wallner, B. Strauss, L. Jandel, and R. W. Lang, ‘A novel methodology for the evaluation of distinctness of image of glossy surfaces’, Prog. Org. Coat., vol. 63, no. 4, pp. 377–381, Nov. 2008, doi: 10.1016/j.porgcoat.2008.06.008.

[4] J. Scheers, M. Vermeulen, C. De Maré, and K. Meseure, ‘Assessment of steel surface roughness and waviness in relation with paint appearance’, Int. J. Mach. Tools Manuf., vol. 38, no. 5–6, pp. 647–656, May 1998, doi: 10.1016/S0890-6955(97)00113-2.

[5] H. Kijima, ‘Mechanism of Roughness Profile Transfer in Skin-pass Rolling of Thin Steel Strip’, 2019.

[6] H. Kijima and N. Bay, ‘Contact conditions in skin-pass rolling’, CIRP Ann. - Manuf. Technol., vol. 56, no. 1, pp. 301–306, 2007, doi: 10.1016/j.cirp.2007.05.070.

[7] H. Kijima and N. Bay, ‘Skin-pass rolling I-Studies on roughness transfer and elongation under pure normal loading’, Int. J. Mach. Tools Manuf., vol. 48, no. 12–13, pp. 1313–1317, Oct. 2008, doi: 10.1016/j.ijmachtools.2008.06.005.

[8] H. Kijima and N. Bay, ‘Skin-pass rolling II-Studies of roughness transfer under combined normal and tangential loading’, Int. J. Mach. Tools Manuf., vol. 48, no. 12–13, pp. 1308–1312, Oct. 2008, doi: 10.1016/j.ijmachtools.2008.06.006.

[9] R. Bünten, K. Steinhoff, W. Rasp, R. Kopp, O. Pawelski, Development of a FEM-model for the simulation of the transfer of surface structure in cold-rolling processes, Journal of Materials Processing Technology, Volume 60 (1–4),1996.

[10] L.J.M. Jacobs, E.H. Atzema, J. Moerman, M.B. de Rooij, ‘Quantification of the influence of anisotropic plastic yielding on cold rolling force’, Journal of Materials Processing Technology, vol. 319, 2023, 118055,

[11] D. J. Wentink, D. Matthews, N. M. Appelman, and E. M. Toose, ‘A generic model for surface texture development, wear and roughness transfer in skin pass rolling’, Wear, vol. 328–329, pp. 167–176, Apr. 2015, doi: 10.1016/j.wear.2015.02.015.

[12] L.J.M. Jacobs, "MODELLING FRICTION IN COLD ROLLING", Ph.D. thesis University of Twente, Enschede. 2025. https://doi.org/10.3990/1.9789036566117

[13] P. Christensen, H. Everfelt, N. Bay, and T. Wanheim, ‘Pressure distribution in plate rolling’, CIRP Ann., vol. 35, no. 1, pp. 141–146, 1986.

[14] J. Jeswiet and W. B. Rice, ‘The neutral zone and temperature at the roll/strip interface’, CIRP Ann., vol. 39, no. 1, pp. 275–277, 1990.

[15] N.A. Fleck, K.L. Johnson, M.E. Mear, and L.C. Zhang, ‘Cold rolling of foil’, Proc. Inst. Mech. Eng. Part B J. Eng. Manuf., vol. 206, no. 2, pp. 119–131, 1992.